Biomedicine & Pharmacotherapy 126 (2020) 109733

Contents lists available at ScienceDirect

Biomedicine & Pharmacotherapy

journal homepage: www.elsevier.com/locate/biopha

Prevent action of magnoflorine with hyaluronic acid gel from cartilage degeneration in anterior cruciate ligament transection induced osteoarthritis

Zhe Cai[a,b,c,1], Ming Hong[d,e,1], Lei Xu[b], Kedi Yang[b], Chentian Li[b], Tianhao Sun[b], Yu Feng[f,*], Huasong Zeng[c,**], William Weijia Lu[b,g,***], Kwong-Yuen Chiu[b,****]

[a] The Joint Center for Infection and Immunity, 1. Guangzhou Institute of Pediatrics, Guangzhou Women and Children's Medical Center, Guangzhou, 510623, China; 2. Institute Pasteur of Shanghai, Chinese Academy of Science, Shanghai, 200031, China
[b] Department of Orthopaedics and Traumatology, Li Ka Shing Faculty of Medicine, The University of Hong Kong, Hong Kong
[c] Department of Allergy, Immunology and Rheumatology, Guangzhou Women and Children's Medical Center, Guangzhou, Guangdong, China
[d] Science and Technology Innovation Center, Guangzhou University of Chinese Medicine, Guangzhou, China
[e] Institute of Clinical Pharmacology, Guangzhou University of Chinese Medicine, Guangzhou, 510000, China
[f] Department of Traumatology, General Hospital of Ningxia Medical University, Yinchuan, Ningxia Hui Autonomous Region, China
[g] Shenzhen Institutes of Advanced Technology, Chinese Academy of Science, Shenzhen, China

ARTICLE INFO

Keywords:
Magnoflorine
Osteoarthritis
Articular cartilage
Subchondral trabecular bone
Hyaluronic acid gel

ABSTRACT

According to the Chinese medicine, magnoflorine exerted significant anti-inflammatory effects and potentially promoted synthesis of proteoglycans in chondrocytes to reverse the progression of rheumatoid arthritis. However, the latent beneficial effect of magnoflorine for the treatment of traumatic osteoarthritis (OA) is still unknown. Therefore, we aim to demonstrate the efficacy of magnoflorine combined with HA-gel in attenuating cartilage degeneration in anterior cruciate ligament transection (ACLT) induced OA rat model. We found that the histological results showed the elevated cartilage matrix, chondrogenic signals and chondroprogenitor cells in HA-gel + magnoflorine treatment. HA-gel + magnoflorine treatment resulted in a decreased modified Mankin's score, and a higher volume ratio of hyaline cartilage (HC)/calcified cartilage (CC) and HC/Sum (whole cartilage), compared to ACLT and HA-gel groups. Furthermore, both the volume ratios of HC/Sum and HC/CC were negatively correlated with modified Mankin's scores. Finally, HA-gel + magnoflorine could significantly increase the BV/TV, Tb.Th, and decrease the Tb.Pf, Po(tot), Conn.Dn and Tb.Sp. *In vitro*, 50 μg/ml magnoflorine treatment could significantly increase the viability, S-phase, migration rate and chondrogenesis of chondroprogenitor cells. There were significant downregulations of MAPK/NF-κB signaling, and upregulations of chondrogenic signals in 50 μg/ml magnoflorine treatment. There were significant downregulations of proinflammatory cytokines and upregulation of IL-10 in HA-gel + magnoflorine treated group. Therefore, our study elucidated a protective effect of HA-gel + magnoflorine on attenuating cartilage degradation and maintaining SCB stabilization in ACLT induced OA.

Abbreviations: HA, hyaluronic acid; AC, articular cartilage; SCB, subchondral bone; OA, osteoarthritis; ACLT, anterior cruciate ligament transection; HC, hyaline cartilage; CC, calcified cartilage; SC, superficial cartilage; Acan, aggrecan; SZ, superficial zone of articular cartilage; MZ, middle zone area of articular cartilage; ECM, extracellular matrix; TCM, traditional Chinese medicine; ROI, Region of Interest; BV/TV, bone volume fraction; Tb.Th, trabecular thickness; Conn.Dn, connectivity density; Tb.Sp, trabecular separation; Tb.Pf, trabecular bone pattern factor; Po(tot), total porosity; Sum, whole cartilage; XTT, Cell Proliferation Kit II; PCR, polymerase chain reaction; Col2a, collagen type II; TNC, tenascin-C; COMP, cartilage oligomeric matrix protein; NF-κB, nuclear factor kappa-light-chain-enhancer of activated B cells; MAPK, mitogen-activated protein kinase; NC, negative control

* Corresponding author at: No. 804, Shengli Street, Department of Traumatology, General Hospital of Ningxia Medical University, Yinchuan, Ningxia, 750004, China. Tel.: +852-5261-9927.
** Corresponding author at: Floor 11, Renmin Middle Road, Department of Allergy, Immunology and Rheumatology, Guangzhou Women and Children's Medical Center, Guangzhou Medical University, Guangzhou, Guangdong, 510120, China. Tel.: +86-020-81330667.
*** Corresponding author at: Room 904, Department of Orthopaedics and Traumatology, The University of Hong Kong, Hong Kong. Tel.: +852-3917-9594.
**** Corresponding author at: Room 216, New Clinical Building, Queen Mary Hospital, Pokfulam, Hong Kong. Tel.: +852-2255-4259.
E-mail addresses: fengyu_7072@163.com (Y. Feng), zenghuasong@gwcmc.org (H. Zeng), wwlu@hku.hk (W.W. Lu), pkychiu@hku.hk (K.-Y. Chiu).
[1] These authors contribute equally to this work.

https://doi.org/10.1016/j.biopha.2019.109733
Received 25 August 2019; Received in revised form 26 November 2019; Accepted 29 November 2019

1. Introduction

Osteoarthritis (OA) is one of the most common types of arthritis characterized by inflammation, abnormal remodeling of subchondral bone (SCB), chronic degeneration of articular cartilage (AC) and osteophyte formation [1]. Significant superficial cartilage (SC) damage, hyaline cartilage (HC) thinning and accelerated SCB resorption are demonstrated in an anterior cruciate ligament transection (ACLT) induced OA rat model, which mimicked human traumatic OA, to assess tissue alterations including type II collagen and aggrecan (Acan) degradation, and chondrocyte loss, which are eventually leading to a progressive OA [2,3].

The interaction between SCB and AC in the pathogenesis of traumatic OA has been drawn attention [4–7], and it is postulated that the pathological changes in the structure and function of SCB play a pivotal role in the OA pathogenesis [8–11], and then influence the integrity and function of AC. The changes in organization and composition of SCB lead to abnormal remodeling in response to the unstable stress states in the progression of OA, and affect the overlying AC adversely [11]. For instance, the abnormal SCB turnover at the osteochondral conjunction may impede molecular communication between bone and cartilage during the development of OA, and may lead to an invasion of calcified cartilage (CC) into middle zone of cartilage (MZ), then finally results in HC thinning [12,13]. The invaded CC is correlated with the chondrocyte hypertrophy, which contributes to the cartilage ossification [14,15]. Therefore, the integrity of AC has been proposed to depend on the biomechanical properties of the underlying SCB [7].

Mechanical stresses caused joint instability is considered to have induced the alterations of biochemical factors which lead to focal degradation of AC in the affected joints [9]. Chondrocytes can sensitively respond to the variation of microenvironment in the joints and regulate the dynamic equilibrium between the synthesis and degradation of cartilage extracellular matrix (ECM), which plays a key role in maintaining the function of cartilage [16]. Due to the erosion of ECM at SC and HC area, this results in a gradual disruption of AC intactness [17], and finally exacerbates the progression of OA. Therefore, the functional changes in chondrocytes play a pivotal role in the AC degeneration, and promoting the proliferation of chondrocytes via proper physical activity stimulation could be one of important strategies for the maintenance of cartilage structure [18].

Recently, most of the classic conservative therapies intended to mitigate pain, which is the most prominent symptoms of OA, rather than modifying this disease. Actually, these therapies in alleviating the progression of OA have limited efficacy, and eventually have led the advanced patients to receive surgical treatments [19]. Thus, there is an unmet requirement for exploring a new treatment to slow down the traumatic OA progression. In clinic, one of the new minimally-invasive therapies to mitigate the joint pain is the intra-articular injection of hyaluronic acid (HA) hydrogels [20]. In addition, hyaluron secreted by the chondrocytes could enhance joint lubrication and helped to prolong the efficacy of growth factors by binding and slowly releasing them as HA-gel degrades [21]. However, clinical studies report that this treatment only provides transient remission of OA symptoms, and the therapeutic efficacy remains ambiguous [22]. Currently, most of the studies engage in enhancing the efficacy of HA hydrogels, such as through combining HA-gel to the traditional Chinese medicine (TCM) for further synergistic therapy of OA [23].

According to the belief in Chinese medicine, magnoflorine is one of the most widely distributed naturally occurring quaternary aporphine alkaloids, and one of key compounds of *Cortex phellodendri* stems (Huang Bo), an effective herb in the TCM formula San-Miao-San, which was used to treat arthritis over hundreds of years [24–26]. Some previous studies demonstrated that magnoflorine exerted significant anti-inflammatory effects, and as the main active ingredient potentially promoted synthesis of proteoglycans in chondrocytes, then reversed the progression of rheumatoid arthritis [27,28]. However, the underlying beneficial effect of magnoflorine on traumatic OA has not been completely investigated. We thereby would study the new role of magnoflorine using the ACLT induced traumatic OA model to illustrate the latent therapeutic effect on attenuating the degeneration of AC by activating the chondrogenic signaling pathway, and by promoting the proliferation, differentiation and migration of chondroprogenitor cells.

2. Material and methods

2.1. Animal model and treatment

The ethics Committee on the Use of Live Animals in Teaching & Research (CULATR) of the University of Hong Kong (HKU) approved all of the protocols (CULATR Ref. No.: 4004-16) and procedures in this study. The standardized surgery of ACLT was made from the medial compartment of right hind limbs of 8-week-old female SD rats and resulted in a true instability-induced OA lesion that mimics OA occurring naturally in human following traumatic injury [29]. After one month of ACLT surgery, the operated rats were randomly divided into 4 groups (HA, HA + Magnoflorine, Magnoflorine and ACLT group, n = 5/group), and received once two weeks in a single dose intra-articular injection with 50 μl of HyStem-HP® HA gel (ESI BIO Products of Ascendance Biotechnology, Alameda, CA, USA) (HA group), 50 μl of HA gel with 100 μg/kg of purified magnoflorine (Purity ≥98 %, HPLC) (Beijing Solarbio Science & Technology Company Limited, Beijing, China) (HA + Magnoflorine group), 50 μl of saline with 100 μg/kg of purified magnoflorine (Magnoflorine group), or no treatment (ACLT group) for 3 consecutive months. The Sham group (n = 5) was received the same operation but without ACLT operation. Then the rats were sacrificed at about 6 month-old to harvest the hind knee joints for micro-CT scans and histopathological analysis.

2.2. Micro-CT analysis

The collected hind knee joints were fixed via 10 % neutral formalin and were scanned using a high resolution micro-CT system (model 1076, SkyScan, Kontich, Belgium). Three hundred and twenty-nine projections for each sample were produced with the following settings: Isotropic voxel 17.3 μm, voltage 100 kV, current 100 mA, and exposure time 320 ms, frame averaging 2, beam filtration filter 1.0 mm aluminum. After scanning, knee joint was reconstructed three-dimensionally by SkyScan NRecon software (version 1.6.8.0, SkyScan). The data sets were then reoriented using DataViewer (version 1.4.4.0, SkyScan) to analyze in the sagittal plane. For analysis of SCB microstructure, a cuboid region was selected as the Region of Interest (ROI) in size of $0.692 \times 0.346 \times 0.346$ mm^3 at the middle of medial tibial plateau under the load bearing area of SCB plate (light blue rectangle area shown in Fig. 4A). The trabecular bone volume fraction (BV/TV, %), connectivity density (Conn.Dn, 1/mm^3), trabecular bone pattern factor (Tb.Pf, 1/mm), total porosity (Po(tot), %), trabecular thickness (Tb.Th, mm) [30], and trabecular separation (Tb.Sp, mm) were measured by the CTAn software (version 1.13.2.1, SkyScan). At least three repeated measurements of each parameter were analyzed.

2.3. Histological examination and modified Mankin's score

The fixed hind knee joints were adequately decalcified and embedded. The slides of central region of the medial tibial plateau were sequentially stained with Toluidine Blue (0.04 % w/v in 0.1 M sodium acetate), Tartrazine solution (0.025 % w/v in 2.5 % acetic acid) and 0.1 % Fast Green solution [3]. According to the modified Mankin's scoring system [31,32], the regions at least from three histologic sections were examined for assessing the grades of the AC structure, cellularity, proteoglycan content, and tidemark intactness. Meanwhile, the volume ratio of HC/ CC, the mean of volume of HC, CC and SC, and the volume ratio of HC/ whole cartilage (Sum) were calculated by Image Pro-Plus

Table 1
Primers' sequences used for quantitative real-time PCR.

Target gene (Accession No.)	Oligonucleotide	Sequence
MAPK (ERK-2) (NM_053842.2)	Forward	5'-ATCCGGGCACCAACCATTGAGC-3'
	Reverse	5'-GTGGTCATTGCTGAGGTGCTGTGT-3'
NF-κB (p105) (NM_001276711.1)	Forward	5'-AACCCATCGCCTTGGCATCCAC-3'
	Reverse	5'-AGTCGAAAAGGGCGTTGGCGT-3'
Col2a (NM_012929.1)	Forward	5'-TGTGCCTCGGAAGAACTG-3'
	Reverse	5'-ATTGGAGCCCTGGATGA-3'
COMP (NM_012834.1)	Forward	5′-GGCTTCATCTTCGGCTAT-3′
	Reverse	5′-CGGGACCTGTAGAGGACTT-3′
TNC (NM_053861.1)	Forward	5′-ACCACAAGAAATAACCCTC-3′
	Reverse	5′-TGTGCCTCGGAAGAACTG-3′
Sox9 (NM_080403.1)	Forward	5′-CACATCAAGACGGAGCAA-3′
	Reverse	5′-TTGTAGTGCGGAAGGTTG-3′
GAPDH (NM_017008.4)	Forward	5′-ATTGTCAGCAATGCATCCTG-3′
	Reverse	5′-ATGGACTGTGGTCATGAGCC-3′

software (version 6.0.0.260, Media Cybernetics, Rockville, MD). At least three sections from 5 samples of each stain were measured for analysis.

2.4. Immunofluorescence staining

According to the previous study [33], the stem cell markers CD44H and CD90 could be used to identify the chondroprogenitor cells in articular cartilage. The slides were direct stained with antibodies FITC anti-rat CD44H (BioLegend, San Diego, CA, USA) and Alexa Fluor® 647 anti-rat CD90 (BioLegend). The number of double positive $CD44H^+CD90^+$ chondroprogenitor cells per tissue area (mm^2) from three repeated stain were quantized.

2.5. Immunohistochemistry staining

The deparaffinized sections were underwent antigen retrieval using Target Retrieval Solution (Dako, Carpinteria, CA). The slides were then quenched in Dako REAL™ Peroxidase-Blocking Solution (Dako) and blocked in 5 % goat serum (Invitrogen, USA) after the incubation of primary antibodies anti-Aggrecan (Acan, 1:50, Abcam, Cambridge, MA), anti-BMP7 (1:100, Abcam), anti-Sox5 (1:100, Abcam), and anti-TGFβ1 (1:100, Abcam) at 4 ˚C overnight. Subsequently, the paraffin sections were incubated with horseradish peroxidase (HRP) conjugated IgG H&L secondary antibody (1:1000, Abcam) for 1 h (h) at room temperature and observed using the liquid 3, 30-diaminobenzidine $(DAB)^+$ substrate-chromogen system (Dako). The number of positive cells per tissue area (mm^2) was counted via Image Pro-Plus software. At least three repeated stain were analyzed.

2.6. Cell culture and treatment

As the previous study described [33], the primary chondroprogenitor cells were isolated from collagenase II digested articular cartilage, and cultured in Dulbecco's modified Eagle's medium (DMEM)/F12 supplemented with 10 % fetal bovine serum (FBS), penicillin (100 U/ml) and streptomycin (100 U/ml) and maintained in a humidified atmosphere of 5 % CO_2 at 37 ˚C.

20 mg magnoflorine was dissolved in 100 μl dimethyl sulfoxide, and then diluted with DMEM/F12 medium into gradient concentrations of 0–100 μg/ml. The cell viability of chondroprogenitor cells treated with gradient concentrations of magnoflorine for 24 and 48 h was assayed by Cell Proliferation Kit II (XTT) (Sigma-Aldrich). The chondrogenesis of chondroprogenitor cells treated with gradient concentrations of magnoflorine for 7–21 days (ds) was stained using 1 % Alcian Blue Solution (Sigma-Aldrich). At least three repeated measurements of each group were analyzed.

2.7. Wound-healing assay

One wound was performed by vertical scratching with a P1000 pipette tip on the monolayer confluent cell at the middle of each well in 6-well plate [34]. The migration rate of chondroprogenitor cells treated with gradient concentrations of magnoflorine in the FBS free DMEM/F12 medium for day 0, 1, 2, 3, 5 and 10 was calculated via the formula as follow.

$$\%\ \text{migration} = \frac{\text{Number of migrated chondrogenic cell}}{\text{Mean of cell number in the same area of wound}} \times 100$$

2.8. Flow cytometry detection

The cultured primary chondroprogenitor cells were direct stained with antibodies FITC anti-rat CD44H (BioLegend) and Alexa Fluor® 647 anti-rat CD90 (BioLegend) to verify the $CD44H^+CD90^+$ chondroprogenitor cells by flow cytometry (FACSCalibur flow cytometer, BD Biosciences Corp., San Jose, CA, USA). The chondroprogenitor cells were collected after gradient concentrations of magnoflorine treatment for 24 h to detect the cell cycle via flow cytometry. At least three repeated measurements of each group were analyzed.

2.9. Quantitative real-time polymerase chain reaction (RT-qPCR)

The extracted total mRNA was quantified by Applied Biosystems® ViiA™ 7 Real Time PCR System (Thermo) using 96-well plate and One Step SYBR® PrimeScript™ RT-PCR kit II (Takara Bio Inc., Otsu, Shiga, Japan). The sequences of the primers NF-κB (p105), MAPK (ERK-2), collagen type II (Col2a), cartilage oligomeric matrix protein (COMP), tenascin-C (TNC), Sox9 and GAPDH (endogenous control) were listed in Table 1. The relative expression of mRNA was measured by the Comparative CT (Threshold Cycle) and calculated by comparing with the expression of GAPDH through the formula $2^{-\Delta Ct}$, where $\Delta Ct = Ct_{target\ gene} - Ct_{GAPDH}$. At least three repeated measurements of each gene were analyzed.

2.10. Luminex multiplex assay

Synovial fluid from each sacrificed rat was harvested and stored at −80 ˚C for subsequent inflammatory cytokines using Luminex Multiplex Assay kit (Merck Millipore, Billerica, MA, USA) with the Bio-Plex 200 suspension array system (Bio-Rad Laboratories, Hercules, CA, USA). At least three repeated measurements of each group were analyzed.

2.11. Statistical analysis

All data were presented as the means ± SEM. Since the sample size was small (n = 5/group in 5 group, 25 in total), Wilcoxon test was performed for comparison between two groups. The comparison of normally distributed variables in different groups was made with one-way analyses of variance (ANOVAs), followed by post hoc Bonferroni's test for comparing the differences and calculating a p value for each pair of comparison. All hypotheses were 2-tailed, and p values < 0.05 were considered significant. Spearman's rank correlation test was used for assessing correlations of continuous variables with skewed distribution. Analyses were performed using GraphPad Prism, Version 6 (GraphPad software, San Diego, CA, USA).

3. Results

3.1. Magnoflorine attenuated cartilage degeneration in ACLT induced OA rat

In ACLT group, a fluctuation with matrix loss and decreased proteoglycan contents were visualized in the superficial zone of cartilage (red arrow pointed area), and even further extended to middle zone (Fig. 1A). The distribution of matrix was heterogeneous with a severe loss of proteoglycan contents in the interterritorial matrix. In addition, we found obviously thicker SZ and obscure tidemark (yellow arrow pointed yellow dash line) in the ACLT group (Fig. 1A). Meanwhile, the modified Mankin's scores was lower in HA + Magnoflorine and Magnoflorine group than ACLT group ($^{###}$ p < 0.0001, $^{&&&}$ p < 0.0001, Fig. 1B). When compared to HA and ACLT groups, the lower volume of CC represented a thinner CC in HA + Magnoflorine group ($^{###}$ p < 0.0001, Fig. 1C). Furthermore, the volume ratio of HC/CC was lower in HA and ACLT groups than HA + Magnoflorine ($^{###}$ p < 0.0001) and Sham groups (*** p < 0.0001), respectively (Fig. 1D). Finally, we found the negative correlations between the modified Mankin's scores with both the volume ratio of HC/CC (r = -0.6735, *** p < 0.0001, Fig. 1E) and the volume ratio of HC/Sum (r = -0.5024, *** p < 0.0001, Fig. 1F). The above results may imply that to maintain the volume of HC was conducive for alleviating OA progression. The decreased volume ratio of HC/CC might be a biomarker for the degeneration of articular cartilage in ACLT induced OA. Therefore, the local administration of HA gel + magnoflorine in the joint space could be a potential treatment for mitigating the decreased volume ratio of HC/CC and even suspend cartilage degeneration.

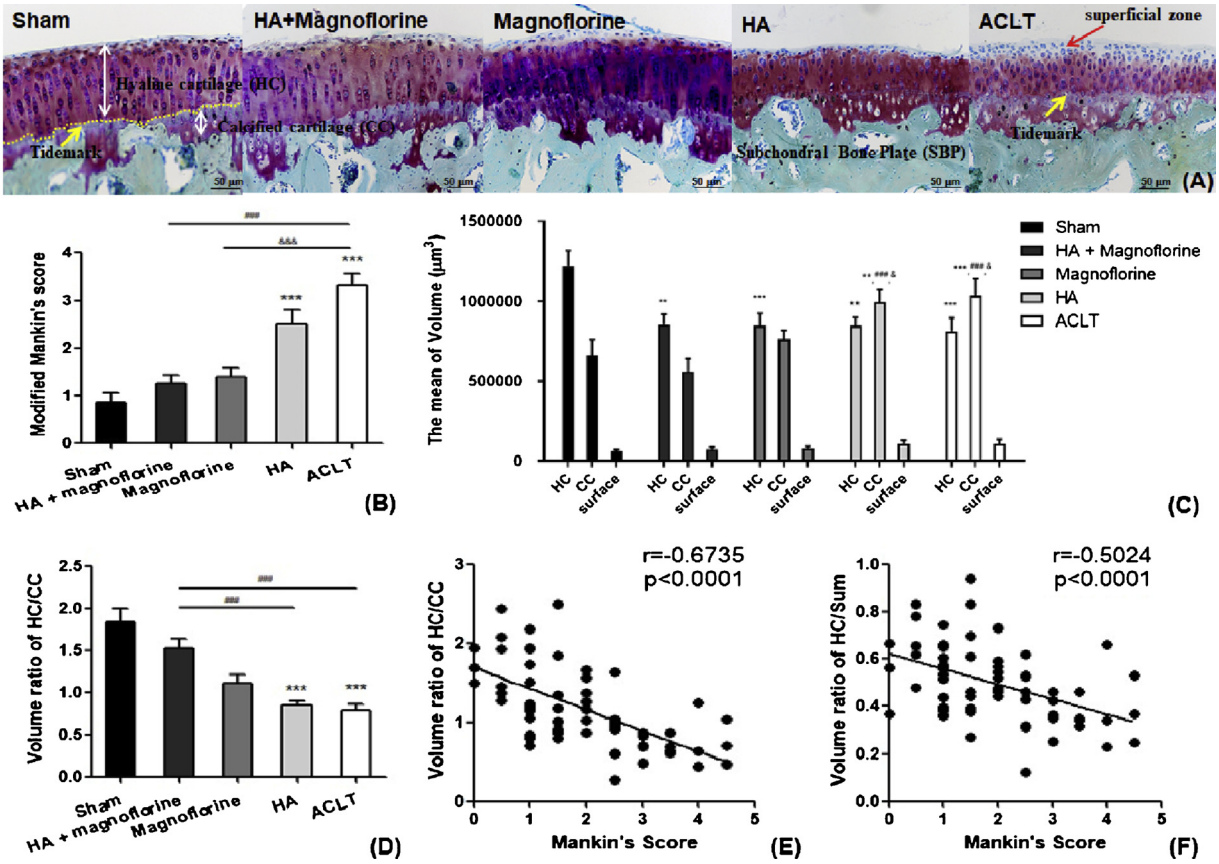

Fig. 1. Histological images and quantitative analysis of rat tibial plateau in different groups. (**A**) The representative images of toluidine blue, tartrazine and fast green stained the tibial medial articular cartilage in different treatment groups. Light blue color stained superficial zone of cartilage (SZ) pointed by the red arrow and the tidemark pointed by the yellow arrow were shown in ACLT and Sham groups, respectively. The white bidirectional arrows pointed the thickness of hyaline cartilage (HC) and calcified cartilage (CC) in the Sham group. Scale bar, 50 μm. (**B**) The Bar charts are shown the modified Mankin's score (n = 5/group, ** p < 0.01, *** p < 0.0001, Sham vs. other groups). Wilcoxon test is used to assess the differences of modified Mankin's score between two groups, $^{###}$ p < 0.0001, HA + Magnoflorine vs. other groups; $^{&&&}$ p < 0.0001, Magnoflorine vs. other groups. (**C**) The Bar charts are shown the quantitative analyzed mean of volume at different zone of cartilage in each group tibial plateau (n = 5, ** p < 0.01, *** p < 0.0001, Sham vs. other groups; $^{##}$ p < 0.01, $^{###}$ p < 0.0001, HA + Magnoflorine vs. other groups; $^{&}$ p < 0.05, $^{&&}$ p < 0.01, Magnoflorine vs. other groups). (**D**) The Bar charts are shown the quantitative analysis of the volume ratio of HC/CC in different treatments (n = 5/group, * p < 0.05, ** p < 0.01). Wilcoxon test is used to assess the differences of the volume ratio of HC/CC between two groups ($^{##}$ p < 0.01, $^{###}$ p < 0.0001, HA + Magnoflorine vs. other groups). (**E-F**) Spearman's rank correlation test is used to assess the correlation. *** p < 0.0001, r = correlation coefficient.

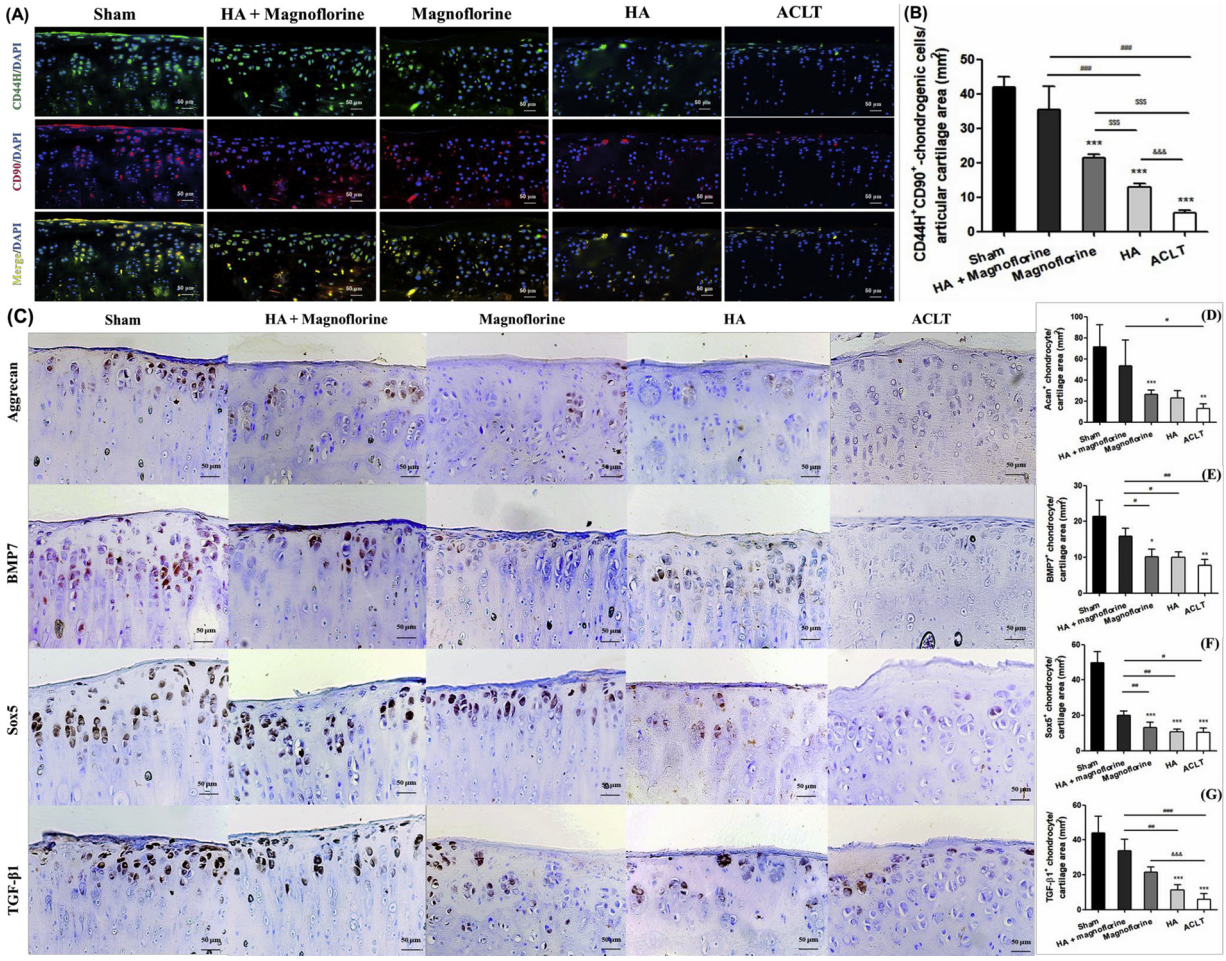

Fig. 2. Immunofluorescence and immunohistochemistry images and quantitative analysis of $CD44H^+CD90^+$ chondrogenic cells and chondrogenic signals in different groups. (**A**) The representative immunofluorescence images of double staining for CD44H (green), CD90 (red) and merged $CD44H^+CD90^+$ chondrogenic cells (co-localization = yellow) at articular cartilage area in different groups. Scale bar, 50 μm. (**B**) The Bar charts are shown the number of $CD44H^+CD90^+$ chondrogenic cells per articular cartilage area (mm^2) in each group (n = 5). Differences among treatments are compared by one-way ANOVA, *** $p < 0.0001$, Sham vs. other groups; $^{\#\#\#}$ $p < 0.0001$, HA + Magnoflorine vs. other groups; $^{\$\$\$}$ $p < 0.0001$, Magnoflorine vs. other groups; $^{\&\&\&}$ $p < 0.0001$, HA vs. other groups). (**C**) The representative images of Aggrecan (Acan)+, BMP7+, Sox5+ and TGF-β1+ chondrogenic cells are shown at articular cartilage area in different groups. Scale bar, 50 μm. The Bar charts are shown the quantitative analysis of the number of (**D**) Acan+, (**E**) BMP7+, (**F**) Sox5+ and (**G**) TGF-β1+ cells per cartilage area (mm^2) in each group, respectively (n = 5). Differences among treatments are compared by one-way ANOVA, * $p < 0.05$, ** $p < 0.01$, *** $p < 0.0001$, Sham vs. other groups; $^{\#}$ $p < 0.05$, $^{\#\#}$ $p < 0.01$, $^{\#\#\#}$ $p < 0.0001$, HA + Magnoflorine vs. other groups; $^{\&\&\&}$ $p < 0.0001$, Magnoflorine vs. other groups.

3.2. Enhancement of chondrogenic signals promoted by HA gel + magnoflorine

In the light of the protective effect on cartilage matrix, there was significantly higher number of double positive $CD44H^+CD90^+$ chondroprogenitor cells at the MZ in HA gel + magnoflorine and Magnoflorine treated rats when compared to HA and ACLT groups ($^{\#\#\#}$ $p < 0.0001$, $^{\$\$\$}$ $p < 0.0001$, Fig. 2A-B). Meanwhile, the quantitative analysis of chondrogenic signaling pathway revealed a significantly higher number of Aggrecan (Acan)+, BMP7+, Sox5+ and TGF-β1+ chondrogenic cells at the SZ and MZ in HA gel + magnoflorine treated rats ($^{\#}$ $p < 0.05$, $^{\#\#}$ $p < 0.01$, $^{\#\#\#}$ $p < 0.0001$, Fig. 2C-G). All the results suggested the elevation of chondrogenic signals reflected an enhanced chondrogenesis due to the HA gel + magnoflorine treatment.

3.3. Anti-inflammatory magnoflorine promoted chondroprogenitor cell proliferation, chondrogenesis and migration in vitro

In vitro study, the isolated chondroprogenitor cell was cultured and confirmed by the double positive staining of chondroprogenitor cell specific biomarkers CD44H and CD90 through flow cytometry assay (blue circle area, Fig. 3A). The cell viability of these chondroprogenitor cells treated with 50 μg/ml magnoflorine for 24 h (*** $p < 0.0001$, Fig. 3B) and 48 h (** $p < 0.01$, Fig. 3C), as well as the frequency of S phase in cell cycle were significantly increased (* $p < 0.05$, Fig. 3F). Meanwhile, no cell toxicity during gradient concentrations of magnoflorine treatment for 48 h was presented (Fig. 3C). In accordance with the results of cell proliferation, the optimal concentration of 50 μg/ml magnoflorine was used to measure the chondrogenesis of chondroprogenitor cell. When compared with no treatment as negative control (NC), there was obvious chondrogenesis with significant high mean ratio of chondrogenic area in 50 μg/ml magnoflorine treatment for 7 ds (*** $p < 0.0001$), 14 ds (* $p < 0.05$) and 21 ds (* $p < 0.05$) detected by Alcian Blue staining shown in Fig. 3G-H. The enhanced chondrogenesis was conducive to the cartilage regeneration. This was confirmed by the activation of the chondrogenic signaling pathway, which was essential for cartilage regeneration. We found the significantly upregulated mRNA expressions of chondrogenic signaling pathway related genes such as *Col2a, COMP, TNC* and *Sox9* in 50 μg/ml magnoflorine treatment than NC (* $p < 0.05$, Fig. 3I). Similarly, there were significant downregulations of *MAPK (ERK-2)* and *NF-κB (p105)* in mRNA expression of 50 μg/ml magnoflorine treated

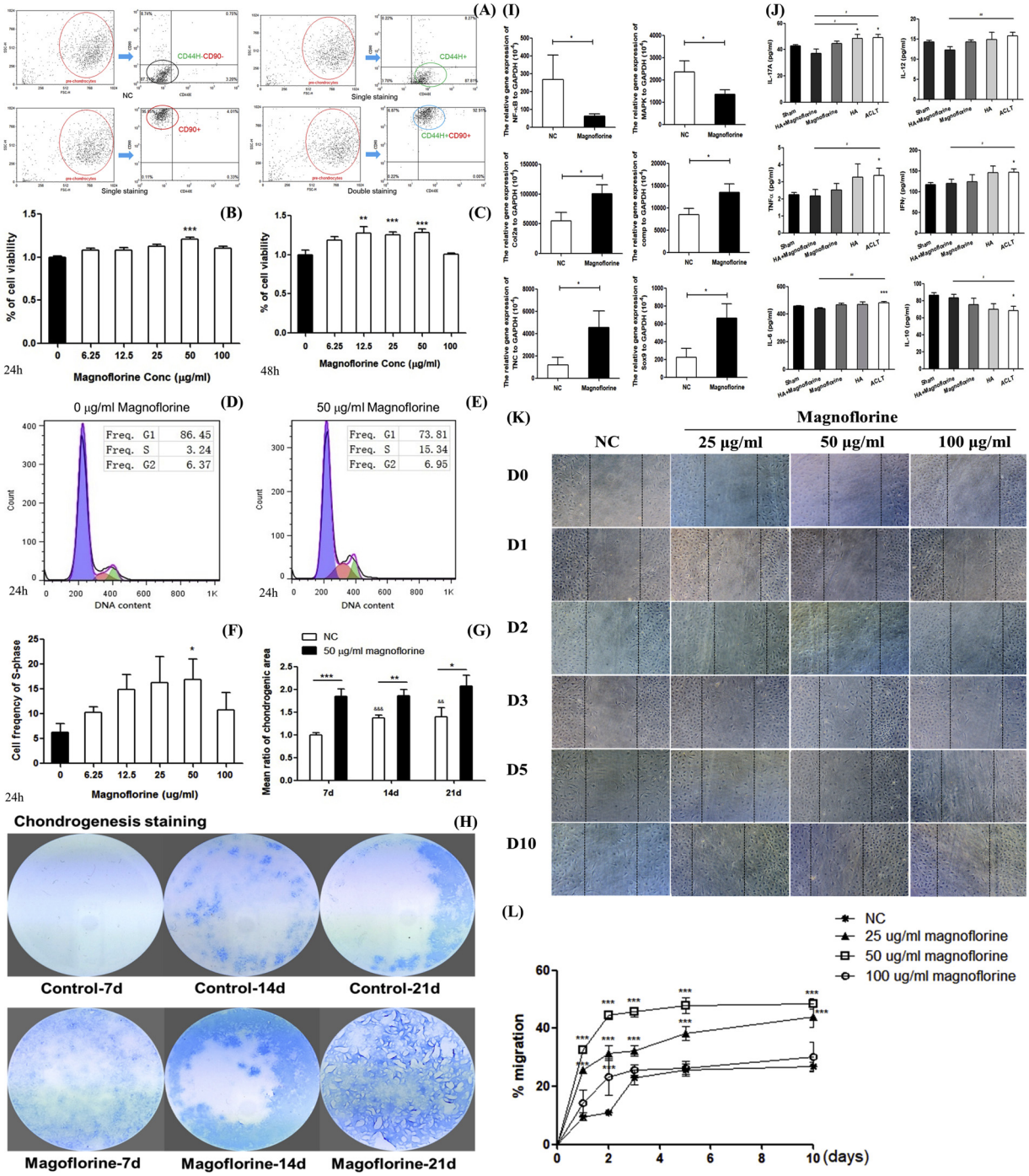

Fig. 3. Anti-inflammatory magnoflorine promoted chondrogenic cell proliferation, chondrogenesis and migration *in vitro*. (**A**) The isolated chondrogenic cells are confirmed using the single or double positive CD44H and CD90 antibodies staining via flow cytometry assay. (**B-C**) The Bar charts are shown the cell viability mean values of chondrogenic cells treated with gradient concentrations of magnoflorine for 24 h and 48 h. Differences among gradient concentrations of magnoflorine vs. no treatment are compared by one-way ANOVA, ** $p < 0.01$, *** $p < 0.0001$. (**D-E**) Flow cytometer detection of chondrogenic cells cycle in null and optimal concentration of 50 μg/ml magnoflorine treatment for 24 h. (**F**) The Bar charts are shown the frequency of S phase in chondrogenic cell cycle with gradient concentrations of magnoflorine treatment for 24 h. Differences among magnoflorine treatments are compared by one-way ANOVA, * $p < 0.05$. (**G**) The Bar charts are shown the mean ratio of chondrogenic area in non-treated negative control (NC) and 50 μg/ml magnoflorine treated chondrogenic cells for 7, 14, and 21 ds. Differences among treated period are compared by two-way ANOVA, $^{\&\&}$ $p < 0.01$, $^{\&\&\&}$ $p < 0.0001$. Wilcoxon test is used to assess the differences of the same period with or without treatment, * $p < 0.05$, *** $p < 0.0001$. (**H**) The representative images of Alcian Blue stained chondrogenic cells chondrogenesis. (**I**) The Bar charts are shown the relative gene expression levels of *NF-κB, MAPK, Col2a, Comp, TNC* and *Sox9* comparing with the expression of *GAPDH* in 50 μg/ml magnoflorine treated chondrogenic cells for 24 h. Differences between magnoflorine treatment and NC are compared by Wilcoxon test, * $p < 0.05$. (J) The Bar charts are shown the levels of synovial fluid cytokines including IL-17A, IL-12, TNF-α, INF-γ and IL-6, & IL-10 from different treated groups. Differences among treatments are compared by one-way ANOVA (* $p < 0.05$, *** $p < 0.0001$; Sham vs. other groups). Wilcoxon test is used to assess the differences between two different treatments. ($^{\#}$ $p < 0.05$, $^{\#\#}$ $p < 0.01$, HA + Magnoflorine vs. other groups). (**K**) The representative images of gradient concentrations of magnoflorine treated chondrogenic cells migration during Day 0 to Day 10. (**L**) The % migration curve is shown the percentage of migrated chondrogenic cells with gradient concentrations of magnoflorine treatment from Day 0 to Day 10. Differences among treatments are compared by one-way ANOVA (** $p < 0.01$, *** $p < 0.0001$; non-treated NC vs. other treatments).

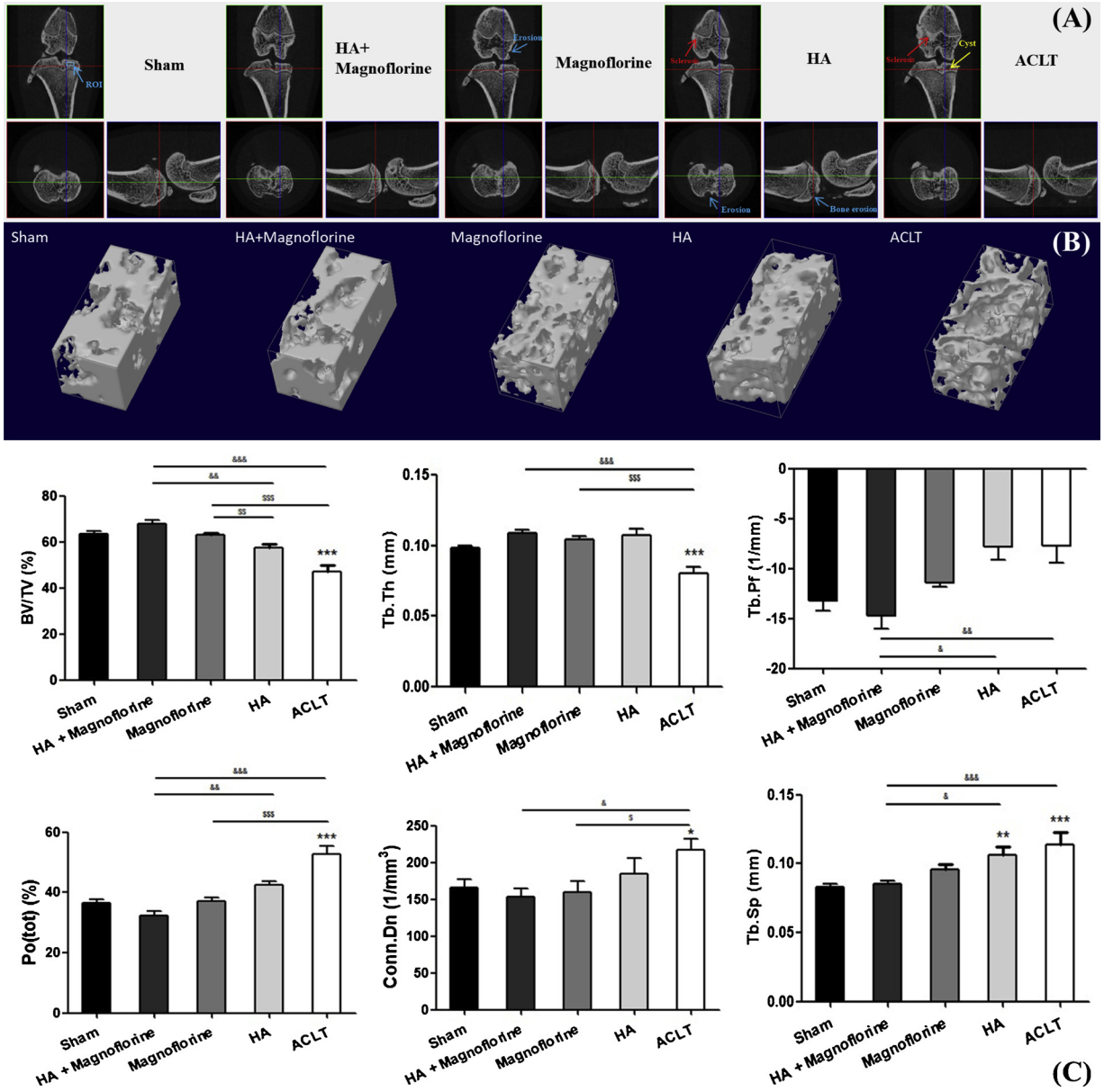

Fig. 4. Micro-architecture of subchondral bone in the ACLT induced OA rats. (**A**) 3-view micro-CT images of the right hind knee joint of rats with different treatment. Blue arrow pointed blue rectangle is shown the region of interest (ROI) in Sham group. Blue arrow pointed bone erosions are shown in Magnoflorine and HA groups. Red arrow pointed bone sclerosis at distal femur epiphyseal is shown in HA and ACLT groups. Yellow arrow pointed medial tibial subchondral bone (SCB) cyst is shown in ACLT group. (**B**) 3D micro-CT reconstruction images of the ROI under the load bearing area of medial tibial SCB from rats with different treatment. (**C**) The Bar charts are shown with the mean values of detailed micro-architectural parameters of medial tibial SCB (n = 5/group). Differences among each parameter are compared by one-way ANOVA. (* $p < 0.05$; *** $p < 0.0001$, Sham vs. other groups). Wilcoxon test is used to assess the differences between two different treatments. ($^{\&}$ $p < 0.05$; $^{\&\&}$ $p < 0.01$; $^{\&\&\&}$ $p < 0.0001$, HA + Magnoflorine vs. other groups; $^{\$}$ $p < 0.05$; $^{\$\$}$ $p < 0.01$; $^{\$\$\$}$ $p < 0.0001$, Magnoflorine vs. other groups).

chondroprogenitor cells (* $p < 0.05$, Fig. 3I). Furthermore, from the results of significantly downregulated pro-inflammatory cytokines including IL-17A, IL-12, TNF-α, INF-γ and IL-6, as well as upregulated anti-inflammatory cytokine IL-10 (* $p < 0.05$, Fig. 3J), we firmly convinced that the magnoflorine could perform a potential anti-inflammatory efficacy. Besides the anti-inflammatory role of magnoflorine, we found a large amount of chondrogenic cells migrated to the wound area (Fig. 3K), and the % migration of chondrogenic cells with 50 μg/ml magnoflorine treatment for 1–10 ds was significant higher than others and NC (*** $p < 0.0001$, Fig. 3L).

3.4. Magnoflorine prevented subchondral bone from un-stabilization in the ACLT induced OA

At 4-month post-surgery, obvious sclerosis of femur epiphyseal plate and lateral cortical bone (red arrow pointed area in Fig. 4A) and trabecular bone cysts (yellow arrow pointed area in Fig. 4A) at the load bearing area of medial tibial plateau from ACLT rats rather than HA gel + magnoflorine treated rats were shown in 3-view and 3D reconstruction images (Fig. 4A-B). Consistent with these appearances, the parameters of subchondral trabecular bone microstructures in HA + Magnoflorine group had a significant increase (Fig. 4C), such as BV/TV ($^{\&\&}$ $p < 0.01$, $^{\&\&\&}$ $p < 0.0001$) and Tb.Th ($^{\&\&\&}$ $p < 0.0001$), and a significant decrease like Tb.Pf ($^{\&}$ $p < 0.05$, $^{\&\&}$ $p < 0.01$), Po(tot) ($^{\&\&}$ $p < 0.01$, $^{\&\&\&}$ $p < 0.0001$), Conn.Dn ($^{\&}$ $p < 0.05$) and Tb.Sp ($^{\&}$

$p < 0.05$, $^{\&\&\&}$ $p < 0.0001$), which implied a protective effect of HA gel + magnoflorine on maintaining the stabilization of trabecular bone microstructure in ACLT induced OA. However, we did not find any statistical differences in these parameters between HA + Magnoflorine and Sham groups. This suggested HA gel + magnoflorine might involve in the resistance of subchondral bone damage in traumatic OA model.

4. Discussion

In the ACLT traumatic OA rat model, SCB undergoes bone remodeling to reply the changes of mechanical stresses environment [23]. Meanwhile, age-dependent biomechanical and biochemical alterations between AC and SCB represent a modulatory role on AC degeneration in ACLT induced OA [35]. In this study, we focused on the possible use of HA gel + magnoflorine to improve current technologies and wished to translate basic studies to clinical application. Particularly, our results have confirmed that local injection of HA gel + magnoflorine in the knee joint capsule implies an indirect preserve effect on maintaining the microstructural integrity of SCB that has strengthened and validated our previous conclusion: a stabilized physiological environment is essential to prevent AC degeneration [7]. The innovation of this study is the evaluation of a chondroprotective effect of magnoflorine on AC degeneration in the ACLT induced OA through enhancing the chondrogenic signals, cell proliferation, migration and cartilage matrix synthesis. Besides we have shown the potential anti-inflammatory effect of HA gel + magnoflorine and possible mechanism of magnoflorine in elevating the chondrogenic signaling.

In the previous study, a decrease of proteoglycan contents and cartilage matrix was illustrated at the SZ of 6-month-old guinea pigs which used as the spontaneous OA model, and was expanded to the MZ in 9-month-old guinea pigs [36]. Moreover, the endochondral ossification of tidemark at the CC layer indicated a pathological exacerbation of OA. Nevertheless, although the detection and analysis of AC were observed in a sole time point in this study, we don't observe an evident loss of cartilage matrix and proteoglycan contents, and do not observe a clear fissure at cartilage area in Sham and HA + Magnoflorine groups rather than ACLT group. All of these are reflected through the results of modified Mankin's scores (Fig. 1D). Contrarily, the significantly higher volume ratio of HC/Sum and HC/CC are both negatively correlated with the modified Mankin's scores (Fig. 1E-F). Therefore, we presume that the magnoflorine may provide a direct protection on maintaining the cartilage matrix and proteoglycan contents of HC. Besides the obvious attenuated deterioration of the cartilage matrix and proteoglycan, we illustrated that there should be an indirect protective effect of magnoflorine on SCB, due to the interaction between SCB and its upper layer AC, even in the relatively unstabilized load bearing status of traumatic OA model. In this study, with the HA gel + magnoflorine treatment, the significantly elevated SCB parameters such as BV/TV and Tb.Th, and the significantly decreased ones like Tb.Pf, Po(tot), Conn.Dn and Tb.Sp reveled that maintaining the stabilization of SCB microstructure, in turn, could indirectly improve the physiological homeostasis in favor of suppressing the cartilage matrix degradation.

On the other hand, the synthesis of cartilage matrix could be induced by TGF-β, especially the expression of aggrecan via the Smad-dependent pathway in chondrogenic cell lines [37]. Otherwise, TGF-β can raise the proliferation of chondrogenic cell and retain the pre-hypertrophic state to suppress the terminal differentiation of chondrocytes [37,38]. In consistent with previous reports, in the present study, the chondrogenic signal levels of Acan, BMP7 and Sox5, as well as the expression of TGF-β1 at the SZ and MZ were significantly increased in HA gel + magnoflorine treatment in ACLT traumatic OA (Fig. 2). Therefore, the HA gel + magnoflorine treatment might elevate the activity of TGF-β1 for chondrogenesis, and promote the $CD44H^+CD90^+$ chondroprogenitor cells proliferation. Even though, few studies have explored the mechanism of magnoflorine in the proliferation and chondrogenesis of chondroprogenitor cells, we have found not only an *in vivo* evidence of chondroprogenitor cells proliferation, but also an in vitro proof that magnoflorine can directly increase the proliferation of primary chondroprogenitor cells and significantly elevate chondrogenesis (Fig. 3A-H).

Furthermore, the MAPK signaling pathway has been found to play a distinct role on the synthesis and homeostasis of cartilage matrix, and the changes of these signaling molecules like p38 and ERK-1/2 perform a prominent role in chondrocyte dysfunction that is reported in the OA pathogenesis and progression [39,40]. During a normal chondrogenesis, suppression of MAPK (ERK-1/2) signaling pathway resulted in a cartilage nodule formation [41]. Similarly, an ERK inhibitor could enhance the expressions of chondrogenic marker genes including Col2a, Acan, COMP and Sox9 [42]. Interestingly, our results presented a significantly downregulated mRNA expressions of MAPK (ERK-2), and upregulated mRNA expressions of Col2a, Comp, TNC and Sox9 in the isolated primary chondroprogenitor cells with 50 μg/ml magnoflorine treatment (Fig. 3I). In addition, the chondrogenesis was increased in the long term differentiation assay (Fig. 3G-H). These results indicated that besides marginal effect on activating the cell cycle of chondroprogenitor cells, magnoflorine could stimulate the chondroprogenitor cells to differentiate to be chondroid tissues through activating the chondrogenic signaling pathway, at least in part, through influencing the MAPK signaling pathway. Meanwhile, regarding to the cartilage, the activated NF-κB regulates the expressions of several matrix degrading enzymes, thus influencing the amount of ECM proteins, and shows indirectly positive effects on the differentiation of terminal chondrocyte [43]. Various stimuli like cytokines, cartilaginous matrix fragments and mechanical stress could induce the synthesis of various cytokines (IL-1β, IL-6, TNF-α, receptor activator of NF-κB ligand) and chemokines (CXCL8) which could mediate NF-κB activation [44–47]. Then the activated NF-κB signaling pathway induces the secretion of various degradative enzymes that lead to the AC further destruction [48,49]. Therefore, inhibiting the NF-κB signaling pathway could impede OA onset and exacerbation. Meanwhile, almost no studies reported the cellular target of magnoflorine in chondroprogenitor cells. Interestingly, our results demonstrated a significant downregulation of NF-κB (p105) in mRNA expression (Fig. 3I), as well as a significant downregulation of pro-inflammatory cytokines such as IL-17A, IL-12, TNF-α, INF-γ and IL-6 in HA gel + magnoflorine treatment (Fig. 3J). Thus, from the results of evident downregulation of transcriptional factors in NF-κB signaling pathway and pro-inflammatory cytokines, the treatment with magnoflorine may rescue the destruction of cartilage in ACLT induced OA. However, more detail mechanisms of magnoflorine in how to affect the MAPK and NF-κB signaling pathways still needs to be further studied.

Clinically, promoting the migration of articular chondroprogenitor cell is a novel strategy for improving cell recruitment into cartilage defects without injuring the subchondral bone plate and for supporting the endogenous repair of degenerated cartilage as a compensatory approach for trauma-affected chondrocyte loss [50]. However, both IL-1β and TNF-α are able to significantly inhibit the migratory activity of primary chondroprogenitor cells, which may contribute to the low regenerative potential of cartilage *in vivo* [50]. This indicates that pro-inflammatory factors have profound influence on the local chondroprogenitor cell recruitment which could compromise the capability of endogenous cartilage repair or in situ regeneration of injured cartilage [50]. Fortunately, from the results of luminex multiplex assay, the production of TNF-α in synovial fluid was significantly decreased. And from wound-healing assay *in vitro*, we have found significantly increased % migration of chondroprogenitor cells with 50 μg/ml magnoflorine treatment for 1–10 ds (Fig. 3K-L). Thus, this founding may imply a possible mechanism of magnoflorine in promoting chondroprogenitor cells differentiation to repair damaged cartilage. This offers a novel potential therapeutic option of magnoflorine for cartilage retrieval via local administration in traumatic OA.

In conclusion, magnoflorine can directly attenuate AC degeneration

through activating the chondrogenic signaling pathway to promote proliferation, chondrogenesis and migration of chondroprogenitor cell in a traumatic OA model. This discovery may provide a potential possibility for promoting and improving chondroprogenitor cell to endogenous repair of cartilage as a clinical therapeutic approach. Meanwhile, the indirect effect on maintaining the integrity of SCB microstructure offers a stabilized physiological environment which is favorable to the cartilage recovery. Moreover, besides a synergistic anti-inflammatory effect, targeting the MAPK and NF-κB signaling pathway by local administration of HA gel + magnoflorine may be a valid clinical prevention strategy for weakening ACLT induced OA progression. We hope our studies could provide a clinical relevant approach using magnoflorine to treat OA in future.

Author contributions

All authors made substantial contributions to study design, analysis and interpretation of data, drafting the manuscript and editing for important intellectual content of this article. Study conception and design: Zhe Cai, William Weijia Lu. Performed the experiments: Zhe Cai, Chentian Li, Kedi Yang, Tianhao Sun. Acquisition of data: Zhe Cai. Contributed reagents/materials/analysis tools: Zhe Cai, Chentian Li, Kedi Yang, Hong Ming, Lei Xu, Yu Feng, Huasong Zeng. Wrote the paper: Zhe Cai, William Weijia Lu, Kwong-Yuen Chiu.

Funding

This work was supported by The Research Grant Council (RGC) Theme-based Research Scheme (TRS) funding (HKUT13-402/17-N), the Research Grant Council of Hong Kong (RGC GRF HKU17206916), and the Shenzhen Peacock Program (No. 110811003586331).

Declaration of Competing Interest

The authors declare that they have no competing interests.

Acknowledgments

We thank all authors' contributions to this study. We thank Mr. Tony Liu, Mr. Boris Chan, Ms. Helen Chan for experimental supports. The authors acknowledge the support from Li Shu Fan Medical Foundation Endowed Professorship in Orthopaedic Surgery.

References

[1] V.B. Kraus, F.J. Blanco, M. Englund, et al., Call for standardized definitions of osteoarthritis and risk stratification for clinical trials and clinical use, Osteoarthr. Cartil. 23 (2015) 1233–1241.
[2] T. Hayami, M. Pickarski, Y. Zhuo, et al., Characterization of articular cartilage and subchondral bone changes in the rat anterior cruciate ligament transection and meniscectomized models of osteoarthritis, Bone 38 (2006) 234–243.
[3] Y. Feng, Z. Cai, W.K. Cheung, et al., Multichromatic TTF staining characterizes cartilage matrix in osteoarthritisand bone development, Histol. Histopathol. 34 (2019) 275–286.
[4] G. Zhen, C. Wen, X. Jia, et al., Inhibition of TGF-beta signaling in mesenchymal stem cells of subchondral bone attenuates osteoarthritis, Nat. Med. 19 (2013) 704–712.
[5] T. Wang, C.Y. Wen, C.H. Yan, et al., Spatial and temporal changes of subchondral bone proceed to microscopic articular cartilage degeneration in guinea pigs with spontaneous osteoarthritis, Osteoarthr. Cartil. 21 (2013) 574–581.
[6] D.B. Burr, M.A. Gallant, Bone remodelling in osteoarthritis, Nat. Rev. Rheumatol. 8 (2012) 665–673.
[7] Z. Cai, Y. Feng, C. Li, et al., Magnoflorine with hyaluronic acid gel promotes subchondral bone regeneration and attenuates cartilage degeneration in early osteoarthritis, Bone 116 (2018) 266–278.
[8] T. Muraoka, H. Hagino, T. Okano, et al., Role of subchondral bone in osteoarthritis development: a comparative study of two strains of guinea pigs with and without spontaneously occurring osteoarthritis, Arthritis Rheum. 56 (2007) 3366–3374.
[9] P. Castrogiovanni, M.D. Rosa, S. Ravalli, et al., Moderate physical activity as a prevention method for knee osteoarthritis and the role of synoviocytes as biological key, Int. J. Mol. Sci. 20 (2019) E511.
[10] M. Ding, A. Odgaard, I. Hvid, Changes in the three-dimensional microstructure of human tibial cancellous bone in early osteoarthritis, J. Bone Joint Surg. Br. 85 (2003) 906–912.
[11] J.S. Day, M. Ding, J.C. van der Linden, et al., A decreased subchondral trabecular bone tissue elastic modulus is associated with pre-arthritic cartilage damage, J. Orthop. Res. 19 (2001) 914-908.
[12] L.A. Setton, W. Zhu, V.C. Mow, The biphasic porovisco-elastic behavior of articular cartilage: role of the surface zone in governing the compressive behavior, J. Biomech. 26 (1993) 581–592.
[13] D.A. Walsh, C.S. Bonnet, E.L. Turner, et al., Angiogenesis in the synovium and at the osteochondral junction in osteoarthritis, Osteoarthr. Cartil. 15 (2007) 743–751.
[14] M. Dougados, X. Ayral, V. Listrat, et al., The SFA system for assessing articularcartilage lesions at arthroscopy of the knee, Arthroscopy 10 (1994) 69–77.
[15] S.L. Yu, P.K. Chan, C.K. Wong, et al., Antagonist-mediated down-regulation of toll-like receptors increases the prevalence of human papillomavirus infection in systemic lupus erythematosus, Arthritis Res. Ther. 14 (2012) R80.
[16] M.A. Szychlinska, R. Imbesi, P. Castrogiovanni, et al., Assessment of vitamin D supplementation on articular cartilage morphology in a young healthy sedentary rat model, Nutrients 11 (2019) E1260.
[17] V. Krenn, L. Morawietz, G.R. Burmester, et al., Synovitis score: discrimination between chronic low-grade and high-grade synovitis, Histopathology 49 (2006) 358–364.
[18] M.A. Szychlinska, P. Castrogiovanni, F.M. Trovato, et al., Physical activity and Mediterranean diet based on olive tree phenolic compounds from two different geographical areas have protective effects on early osteoarthritis, muscle atrophy and hepatic steatosis, Eur. J. Nutr. 58 (2019) 565–581.
[19] R.L. Taruc-Uy, S.A. Lynch, Diagnosis and treatment of osteoarthritis, Prim. Care 40 (2013) 821–836.
[20] E. Losina, A.M. Weinstein, W.M. Reichmann, et al., Lifetime risk and age at diagnosis of symptomatic knee osteoarthritis in the US, Arthritis Care Res. (Hoboken) 65 (2013) 703–711.
[21] E. Kon, R. Buda, G. Filardo, et al., Platelet-rich plasma: intra-articular knee injections produced favorable results on degenerative cartilage lesions, Knee Surg. Sports Traumatol. Arthrosc. 18 (2010) 472–479.
[22] A. Egemen, K. Hayrettin, A. Isik, Intraarticular injections (corticosteroid, hyaluronic acid, platelet rich plasma) for the knee osteoarthritis, World J. Orthop. 5 (2014) 351–361.
[23] Z. Cui, J. Crane, H. Xie, et al., Halofuginone attenuates osteoarthritis by inhibition of TGF-β activity and H-type vessel formation in subchondral bone, Ann. Rheum. Dis. 75 (2016) 1714–1721.
[24] Z. Cai, C.K. Wong, J. Dong, et al., Anti-inflammatory activities of Ganoderma lucidum (Lingzhi) and San-Miao-San supplements in MRL/lpr mice for the treatment of systemic lupus erythematosus, Chin. Med. 11 (2016) 23.
[25] D.P. Chen, C.K. Wong, P.C. Leung, et al., Anti-inflammatory activities of Chinese herbal medicine sinomenine and Liang Miao San on tumour necrosis factor-α-activated human fibroblast-like synoviocytes in rheumatoid arthritis, J. Ethnopharmacol. 137 (2011) 457–468.
[26] Y.X. Bao, C.K. Wong, E.K. Li, et al., Immunomodulatory effects of Lingzhi and San-Miao-San supplementation on patients with rheumatoid arthritis, Immunopharmacol. Immunotoxicol. 28 (2006) 197–200.
[27] Y. Gui, X. Qiu, Y. Xu, et al., Bu-Shen-Ning-Xin decoction suppresses osteoclastogenesis via increasing dehydroepiandrosterone to prevent postmenopausal osteoporosis, Biosci. Trends 9 (2015) 169–181.
[28] R. Yue, L. Zhao, Y. Hu, et al., Metabolomic study of collagen-induced arthritis in rats and the interventional effects of Huang-Lian-Jie-Du-Tang, a traditional Chinese medicine, Evid. Based Complement. Alternat. Med. 2013 (2013) 439690.
[29] S. Giunta, A. Castorina, R. Marzagalli, et al., Ameliorative effects of PACAP against cartilage degeneration. Morphological, immunohistochemical and biochemical evidence from in vivo and in vitro models of rat osteoarthritis, Int. J. Mol. Sci. 16 (2015) 5922–5944.
[30] M. Hahn, M. Vogel, M. Pompesius-Kempa, et al., Trabecular bone pattern factorea new parameter for simple quantification of bone microarchitecture, Bone 13 (1992) 327–330.
[31] V.B. Kraus, J.L. Huebner, J. DeGroot, et al., The OARSI histopathology initiative e recommendations for histological assessments of osteoarthritis in the guinea pig, Osteoarthr. Cartil. 18 (2010) S35–52.
[32] M.A. Szychlinska, F.M. Trovato, M.D. Rosa, et al., Co-expression and co-localization of cartilage glycoproteins CHI3L1 and Lubricin in osteoarthritic cartilage. Morphological, immunohistochemical and gene expression profile, Int. J. Mol. Sci. 17 (2016) 359.
[33] W. Tong, Y. Geng, Y. Huang, et al., In vivo identification and induction of articular cartilage stem cells by inhibiting NF-κB signaling in osteoarthritis, Stem Cells 33 (2015) 3125–3137.
[34] A. Zaritsky, Y.Y. Tseng, M.A. Rabadán, et al., Diverse roles of guanine nucleotide exchange factors in regulating collective cell migration, J. Cell Biol. 216 (2017) 1543–1556.
[35] R.J. Lories, F.P. Luyten, The bone-cartilage unit in osteoarthritis, Nat. Rev. Rheumatol. 7 (2011) 43–49.
[36] W. Zhao, T. Wang, Q. Luo, et al., Cartilage degeneration and excessive subchondral bone formation in spontaneous osteoarthritis involves altered TGF-β signaling, J. Orthop. Res. 34 (2016) 763–770.
[37] T.F. Li, R.J. O'Keefe, D. Chen. TGF-beta signaling in chondrocytes, Front. Biosci. 10 (2005) 681–688.
[38] P.M. van der Kraan, E.N. Blaney Davidson, A. Blom, et al., TGF-beta signaling in chondrocyte terminal differentiation and osteoarthritis: modulation and integration of signaling pathways through receptor, Smads. Osteoarthr. Cartil. 17 (2009) 1539–1545.

[39] I. Prasadam, S. van Gennip, T. Friis, et al., ERK-1/2 and p38 in the regulation of hypertrophic changes of normal articular cartilage chondrocytes induced by osteoarthritic subchondral osteoblasts, Arthritis Rheum. 62 (2010) 1349–1360.
[40] I. Prasadam, T. Friis, W. Shi, et al., Osteoarthritic cartilage chondrocytes alter subchondral bone osteoblast differentiation via MAPK signalling pathway involving ERK1/2, Bone 46 (2010) 226–235.
[41] C.D. Oh, S.H. Chang, Y.M. Yoon, et al., Opposing role of mitogen-activated protein kinase subtypes, erk-1/2 and p38, in the regulation of chondrogenesis of mesenchymes, J. Biol. Chem. 275 (2000) 5613–5619.
[42] D.H. Rosenzweig, S.J. Ou, T.M. Quinn, P38 mitogen-activated protein kinase promotes dedifferentiation of primary articular chondrocytes in monolayer culture, J. Cell. Mol. Med. 17 (2013) 508–517.
[43] E. Mariani, L. Pulsatelli, A. Facchini, Signaling pathways in cartilage repair, Int. J. Mol. Sci. 15 (2014) 8667–8698.
[44] C.R. Scanzello, S.R. Goldring, The role of synovitis in osteoarthritis pathogenesis, Bone 51 (2012) 249–257.
[45] S.C. Liu, C.J. Hsu, H.T. Chen, et al., CTGF increases IL-6 expression in human synovial fibroblasts through integrin-dependent signaling pathway, PLoS One 7 (2012) e51097.
[46] C.H. Hou, C.H. Tang, C.J. Hsu, et al., CCN4 induces IL-6 production through alphavbeta5 receptor, PI3K, Akt, and NF-kappaB singling pathway in human synovial fibroblasts, Arthritis Res. Ther. 15 (2013) R19.
[47] L. Xing, L. Carlson, B. Story, et al., Expression of either NF-kappaB p50 or p52 in osteoclast precursors is required for IL-1-induced bone resorption, J. Bone Miner. Res. 18 (2003) 260–269.
[48] S. Krasnokutsky, M. Attur, G. Palmer, et al., Current concepts in the pathogenesis of osteoarthritis, Osteoarthr. Cartil. 16 (2008) S1–3.
[49] M.B. Goldring, K.B. Marcu, Cartilage homeostasis in health and rheumatic diseases, Arthritis Res. Ther. 11 (2009) 224.
[50] H. Joos, A. Wildner, C. Hogrefe, et al., Interleukin-1 beta and tumor necrosis factor alpha inhibit migration activity of chondrogenic progenitor cells from non-fibrillated osteoarthritic cartilage, Arthritis Res. Ther. 15 (2013) R119.